Research Article | Vol. 27, No. 26 / 23 December 2019 / Optics Express 37419
Optics EXPRESS

1D moiré shapes by superposed layers of micro-lenses

THOMAS WALGER,[1,*] THÉOPHANE BESSON,[1] VALENTIN FLAURAUD,[1] ROGER D. HERSCH,[2] AND JUERGEN BRUGGER[1]

[1]*Microsystems Laboratory, École Polytechnique Fédérale de Lausanne (EPFL), CH-1015 Lausanne, Switzerland*
[2]*School of Computer and Communication Sciences, École Polytechnique Fédérale de Lausanne (EPFL), CH-1015 Lausanne, Switzerland*
[*]*thomas.walger@epfl.ch*

Abstract: Two superposed layers of transparent cylindrical lenslet gratings create classical moiré fringes, when illuminated from behind. We rely on this observation to conceive special devices made of superposed lenslet gratings that produce animated moirés when they are tilted against the light. One-dimensional moirés can show a message moving back and forth along a given direction or radially expanding towards the exterior of a disk. These 1D moirés are conceived by fabricating two layers of micro-lenses on both sides of a transparent substrate. The top layer is a rectilinear grating of cylindrical lenslets and the bottom layer is an arrangement of smaller lenslets of different sizes and orientations that create a high contrast. Moirés created by superpositions of lenslets are visually striking and can be challenging to fabricate. Therefore they have a high potential for art, decoration, and document security.

1. Introduction

The superposition of layers incorporating repetitive structures yields intriguing visual effects. Certain types of superpositions, known as moiré fringes, are well known from daily life, such as the moiré fringes between bridge railings or between curtain folds in front of a window. Moiré effects are generally undesirable: artefacts in scanning and printing are often due to interferences between periodic structures. In contrast, artists and scientists synthesize moiré shapes in order to produce interesting visual effects [1–3].

Moiré effects are especially attractive because, when superposed, layers incorporating very tiny structures yield macroscopic shapes. These moiré shapes may move or change upon relative displacement of the layers. When produced at very high resolution, these layers cannot be copied by simple means and therefore offer a high protection against counterfeiting attempts [4]. Devices relying on moving 2D moiré shapes combining visual attractiveness and counterfeit prevention are starting to be widely used as security threads for banknotes [5].

In the present contribution, the new approach we propose for the creation of moiré shapes relies on two layers of lenslets (Fig. 1(a)). We noticed that the superposition of two layers of lenticular gratings yields moiré fringes that have the same layout as the moiré fringes produced by the superposition of two gratings of lines imaged on transparencies (Fig. 2(a)). Relying on this observation, we developed approaches to create cylindrical lenslet arrays that are arranged in the same manner as the printed patterns used for the creation of different types of moirés (Fig. 1(b)). Hereby, the top layer of lenslets, called revealing layer, behaves as the sampling layer, similar to the transparent lines of a grating printed on a transparent sheet. The bottom lenslet layer forms the base layer, which in the case of a 1D moiré [3], comprises an array of repeated tiny shapes that are formed by the contrast between different types of lenslets.

#376132 https://doi.org/10.1364/OE.27.037419
Journal © 2019 Received 3 Oct 2019; revised 9 Nov 2019; accepted 18 Nov 2019; published 11 Dec 2019

Optics EXPRESS

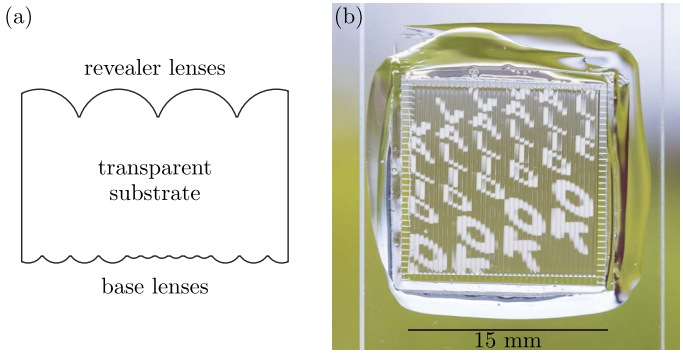

Fig. 1. (a) Schematic cross-section of the new 1D moiré samples. (b) Photograph of a fabricated sample depicting a "Valid OK" 1D moiré, illuminated from an office window with plants and sky in the background (see Visualization 1). The revealer is made of a rectilinear vertical cylindrical lenslet grating of period 400 µm. The inside of the characters is filled with a grating of horizontal cylindrical lenslets of period 16 µm. The outside of the characters is filled with a grating of vertical cylindrical lenslets of period 6 µm.

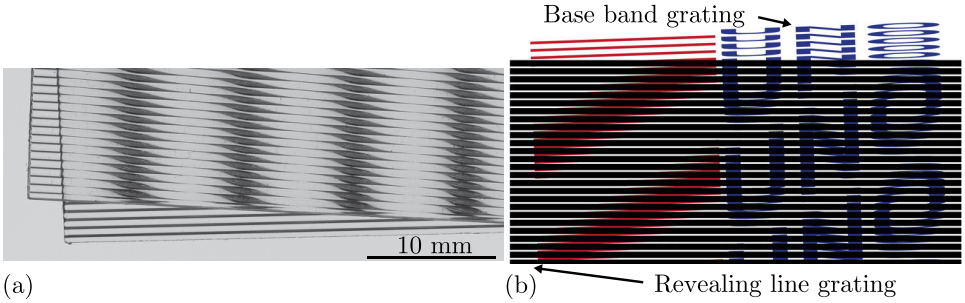

Fig. 2. (a) Photograph of moiré fringes produced by the superposition of two layers of lenticular gratings. (b) Example of a 1D moiré formed by repetitive base bands superposed with a sampling revealing line grating [3].

2. Background

The simplest type of moiré is the moiré fringes produced by the superposition of two line gratings. When displacing one layer on top of the other, the resulting moiré fringes move. The orientations and periods of various types of moirés were first studied by analyzing the geometry of the superposed layers in the spatial domain [6–8].

2.1. Moiré fringes

Orientations, periods as well as the moiré intensity profile of moiré fringes can also be modeled by considering the superposition of the layers as a multiplication in the spatial domain, and therefore as a convolution in the spatial frequency domain [9], [[10], Chap. 2 and 4]. Figure 3 shows two raised cosinusoidal gratings at different orientations in the image plane (x, y), their representation in the 2D frequency plane (u, v), their superposition, as well as the convolution of their frequencies. The convolution yields in the spatial frequency space both a new additive $(\vec{f}_1 + \vec{f}_2, -\vec{f}_1 - \vec{f}_2)$ and a new subtractive moiré $(\vec{f}_1 - \vec{f}_2, \vec{f}_2 - \vec{f}_1)$.

The subtractive moiré is the most visible, i.e. the moiré whose first harmonic frequency is obtained by subtracting the first harmonic frequency of one layer from the first harmonic

Optics EXPRESS

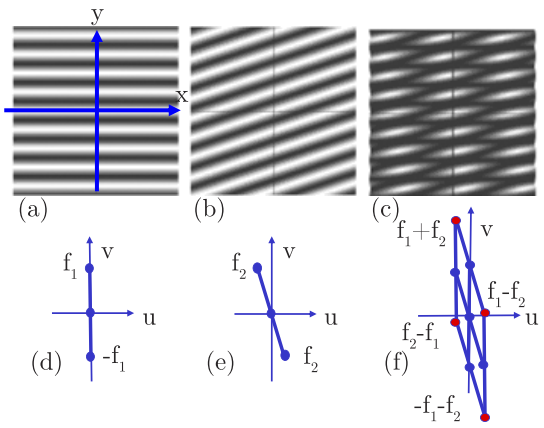

Fig. 3. Top (a) and (b): raised cosinusoidal gratings and (c) their multiplicative superposition in the image domain. Bottom (d) and (e): impulse pairs obtained by the Fourier transform of the corresponding individual layers and (f) the new additive and subtractive impulse pairs obtained by convolution of the frequency pairs $(\vec{f_1}, -\vec{f_1})$ and $(\vec{f_2}, -\vec{f_2})$.

frequency of the second layer [[10], pp. 9-30]. Nearly all additive moirés and higher order moirés are either not strong enough or their frequency is too high to be visible.

Moirés are defined by their geometric layout (orientation and period) and by their intensity profile. In the spectral domain, the geometric layout is given by the location of the moiré frequencies (e.g. in Fig. 3(f), the impulses $(\vec{f_1} - \vec{f_2}, \vec{f_2} - \vec{f_1})$). The intensity profile of the moiré is defined by the amplitude of its harmonic components obtained by the convolution of the frequency components of the two gratings, i.e. by multiplying the amplitudes of the corresponding contributing impulses. In the case of two cosinusoidal gratings given by frequencies $\pm\vec{f_1}$ and $\pm\vec{f_2}$, with respective amplitudes a_1 and a_2, the cosinusoidal moiré frequencies $(\vec{f_1} - \vec{f_2}, \vec{f_2} - \vec{f_1})$ have the amplitude $a_m = a_1 \cdot a_2$. The multiplication of the amplitudes of the Fourier components of the two gratings corresponds, in the image domain, to a convolution operation. Therefore, the moiré intensity profile is determined by the cyclic convolution operation of the normalized first grating and the normalized second grating [[10], Chap. 4, pp. 81-107].

2.2. 1D Moiré

The 1D moiré is more sophisticated than the moiré fringes that are obtained with a revealing layer sampling a grating of lines (Fig. 2(b), red stripes). To produce a 1D moiré, the base layer is formed by replicated bands whose content varies in two dimensions (Fig. 4). In contrast to 2D moirés [11,12], the 1D moiré base bands are replicated only along a single direction. The base bands incorporate the same information as the resulting desired moiré shapes, but compressed along one direction (Fig. 2(b), vertically-compressed "UNO" letters). Along the other direction one is free to place as many symbols or letters as desired.

There is a linear relation between the content of a base band and the 1D moiré resulting from the sampling action of the revealing layer (Fig. 4). For a base-band replication vector $\vec{t} = (t_x, t_y)$ and a revealing layer period T_r, the linear mapping from base-band space to moiré space is the following:

$$\begin{bmatrix} x \\ y \end{bmatrix} = \begin{bmatrix} 1 & \frac{t_x}{T_r - t_y} \\ 0 & \frac{T_r}{T_r - t_y} \end{bmatrix} \cdot \begin{bmatrix} x' \\ y' \end{bmatrix} \tag{1}$$

Optics EXPRESS

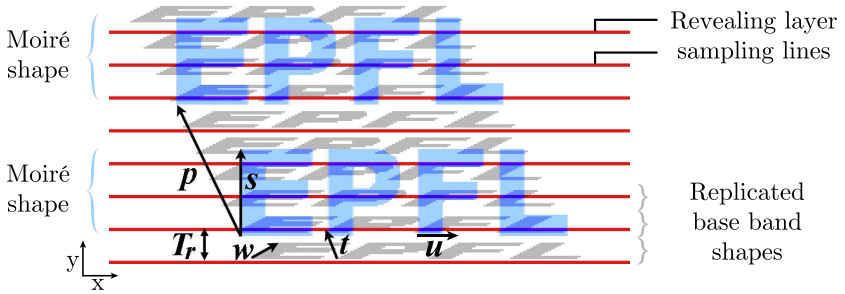

Fig. 4. Representation of the base bands (gray) replicated by vector $\vec{t}$, of the revealing layer sampling line grating (red) having period T_r as well as the corresponding vertically-orientated (vector $\vec{s}$) moiré letters (blue) laid out horizontally (vector $\vec{u}$) replicated along vector $\vec{p}$.

where (x', y') are base-band coordinates and (x, y) are the corresponding moiré coordinates. This linear mapping is easy to derive by relying on the geometry of the moiré in image space [3].

For example, by mapping the base-band repetition vector $\vec{t} = (t_x, t_y)$, one obtains the moiré repetition vector $\vec{p} = (p_x, p_y)$, along which the moiré moves when displacing the revealing layer on top of the base layer. Furthermore, to ensure vertically-oriented moiré letters (Fig. 4), one needs to map the vector $\vec{s}$ representing the vertical of the capital moiré letters into the vector $\vec{w}$ that represents the slanted letters that have to be generated within the base bands. Since this mapping is from moiré space to base-layer space, it is defined by the inverse of the matrix given in Eq. (1).

The mapping between base band positions (x', y') and moiré band positions (x, y) according to Eq. (1) is limited to linear moiré, i.e. moiré produced by rectilinear base bands sampled by a rectilinear revealing line grating or lenticular grating. In the case that the base bands are subject to a first non-linear geometric transformation and the revealing grating is subject to a second non-linear geometric transformation, the resulting moiré is in general a non-linear transformation of the rectilinear moiré that would have been obtained by having the non-transformed revealing grating sampling the non-transformed base band grating.

Expressed in mathematical terms, Hersch and Chosson [3] have shown that there is a simple relation between the moiré transformation $\{m_x(x_t, y_t), m_y(x_t, y_t)\}$, the base layer transformation $\{h_x(x_t, y_t), h_y(x_t, y_t)\}$ and the revealing layer transformation $\{g_x(x_t, y_t), g_y(x_t, y_t)\}$ which respectively map target space locations (x_t, y_t) to original space locations (x, y).

This relation is given by the following equations:

$$\begin{aligned} x = m_x(x_t, y_t) &= h_x(x_t, y_t) + \big(h_y(x_t, y_t) - g_y(x_t, y_t)\big) \cdot \frac{t_x}{T_r - t_y} \\ y = m_y(x_t, y_t) &= h_y(x_t, y_t) \cdot \frac{T_r}{T_r - t_y} - g_y(x_t, y_t) \cdot \frac{t_y}{T_r - t_y} \end{aligned} \tag{2}$$

where T_r is the period of the horizontal revealing layer grating and (t_x, t_y) is the replication vector of the horizontal base bands in the original space, i.e. in the space before transformation into the target space (x_t, y_t). An example of such transformations is given in Section 6.

3. Related work

Layers forming moiré effects need not necessarily be composed of gratings of lines. The base layer may be formed by small repetitive squares incorporating a 2D micro-image [11,13]. Properties of the 2D repetitive moiré resulting from the superposition of an array of 2D micro-images and a 2D array of tiny holes or micro-lenses have been analyzed in the Fourier domain [14].

Optics EXPRESS

Lebanon and Bruckstein [2] consider moiré fringes created by two superposed gratings. Their goal is to obtain a given maximally-visible moiré by applying a variational approach yielding successive modifications of the implicit functions determining the layouts of the superposed base and revealing layer gratings. Chosson and Hersch [15] investigated the creation of level-line moirés. They showed how to hide two motives within a single base layer and reveal them with two differently-oriented revealing layers. In these previous works on moirés, the revealing layer is considered to be a sampling layer. It can be implemented by gratings of transparent lines on a black film or by lenticular arrays. The configuration of two-dimensional micro-lens arrays sampling the underlying base layer micro-images were analyzed by Mikami [13], Hutley et al. [11] and Kamal et al. [12]. One-dimensional cylindrical lens arrays sampling 1D base layer structures were conceived and analyzed by Cadarso et al. [4]. Further reflective 1D samples were conceived and produced by Zheng et al [16]. However, no previous work mentions the possibility of forming moirés by superposed layers of lenslets. In a concurrent submission, the authors of the present paper demonstrate how to generate level-line moirés with two superposed layers of cylindrical lenslets [17]. In the present work, the authors show how to generate 1D moiré effects by fabricating a revealing layer and a base layer on both sides of a transparent substrate. The revealer is made of cylindrical lenses and is superposed with the base, which is formed by arrays of small lenses that cover the base-layer shapes.

4. Design

As explained in Section 2, to obtain 1D moirés, a revealer and a base must be created. The revealer is an array of cylindrical micro-lenses that samples lines on the base, located in their focal plane. In traditional 1D moiré technology, the replicated base bands are printed on paper or directly at the back of the lenticular revealer. The different colors or intensities that appear on the printed base (Fig. 2(b)) are now replaced by different lens structures. Within each band of the base layer, the contrast is created for example by conceiving small focusing cylindrical lenslets on the interior parts of the shapes and by conceiving diffusively-transmitting randomly-placed spherical lenslets of varying sizes on the exterior parts (Fig. 5). Depending on the desired effect, the structures in the base can be light-focusing, light-diffusing or diffractive.

The revealing layer is made of a cylindrical lenslet grating sampling the base layer gratings. A section through the transparent element comprising base and revealing gratings is shown in Fig. 6. In that example, at a normal viewing orientation, the revealing layer lenslets sample a base band portion that represents the exterior of the base band shape. In this exterior region, randomly-positioned small spherical lenses of various sizes diffuse the light from several directions into the eye. When the viewing angle is changed, the revealing layer lenslets sample a region interior to the base band shape and capture light that has been focused by the base layer lenses and therefore comes from a specific angle towards the observer. This change from diffuse light to directed light creates the desired contrast. Sharp moirés are obtained when the revealer lenslets focus on the base layer.

The parameters defining the revealing layer lenslets are the repetition period (pitch) T_r, the width of the cylindrical lenslet w_r, their sag-height h_r and their focal length f_r. These lens parameters can be calculated by considering a section of a generic cylindrical lenslet (Fig. 7(b)).

We rely on the laws of geometrical optics [18] and make the approximation that a circular section of the cylindrical lenslet is capable of focusing parallel incident light into a focal point. Let us calculate the relations between the different lens parameters.

By relying on the geometry of Fig. 7(b), we have :

$$(R - h)^2 = R^2 - (w/2)^2 \tag{3}$$

Optics EXPRESS

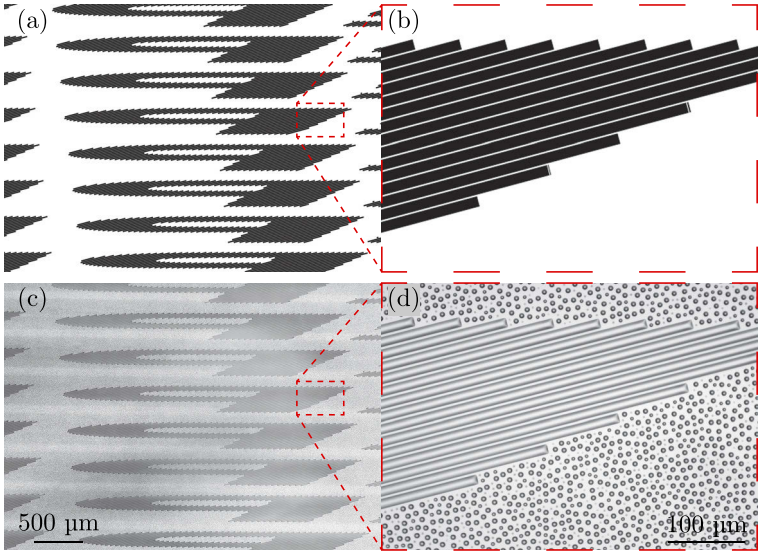

Fig. 5. (a) Bitmap showing the interior and exterior of the compressed letter shape "P" within successive base bands with black segments forming the interior of the letter shapes, to be filled with cylindrical lenslets. The letters are mirrored in the base to obtain the correctly-oriented text when looking through the revealer. (b) Magnified area of the bitmap image. (c) Optical micrograph of the fabricated lenslet base layer. The depicted area corresponds to the design area shown in (a). (d) Magnified area of (c) that corresponds to the design area shown in (b). The rectilinear cylindrical lenslets have a repetition period of 16 µm and are laid out at 15° within the interior regions of the letter shapes. Randomly-placed spherical lenslets of diameters varying between 4 µm and 7 µm are laid out in the exterior regions.

and by developing Eq. (3) in order to express the lens radius R as a function of the lens width w and the cap-height h, we obtain

$$R = \frac{w^2}{8h} + \frac{h}{2} \tag{4}$$

The focal length is given by [[18], formula 5.10]:

$$f = \frac{n_S}{n_S - n_{air}} R \tag{5}$$

where n_S and n_{air} are the indices of refraction of the lens substrate and of the air, respectively. In the case of a material having an index of refraction of 1.5, we obtain the simple relation $f = 3R$.

Note the relation between focal length f, the mono-lens substrate thickness d and the sag-height h:

$$h = f - d \tag{6}$$

In many cases, input parameters are the thickness d of the chosen substrate and the lens width w, which is often the lens repetition period (also called lens pitch). With Eqs. (4), (5), and (6) and by the change of variable $m = n_s/(n_s - n_{air})$ we obtain the following relation between lens radius R, thickness d and lens width w:

$$R^2 \cdot 4m(m-2) + R \cdot 8d(1-m) + w^2 + 4d^2 = 0 \tag{7}$$

Optics EXPRESS

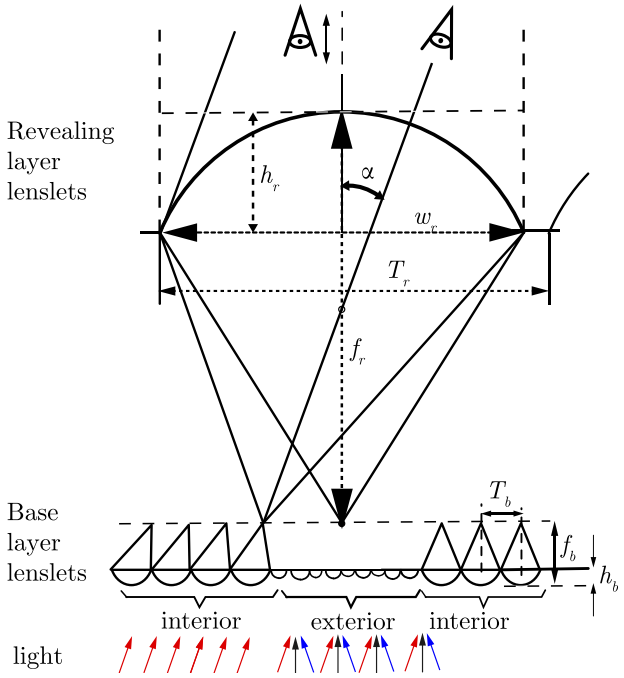

Fig. 6. Section through the transparent element comprising on one side a cylindrical lens that is part of the revealing sampling layer and on the other side a base band with both small cylindrical lenses forming the interior of the base band shapes and smaller randomly-placed spherical lenses of various sizes forming the exterior of the base band shapes.

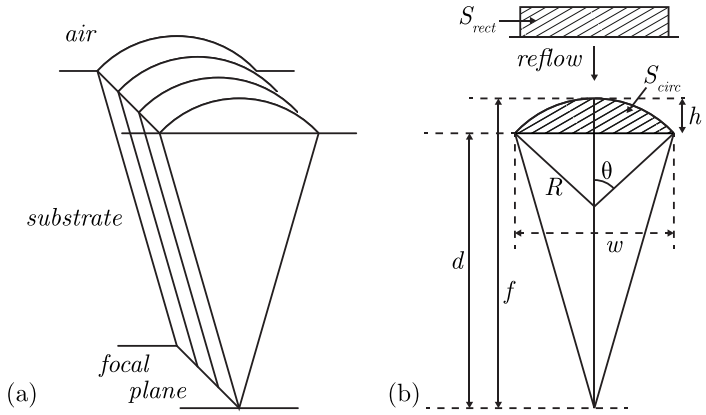

Fig. 7. (a) Part of a cylindrical lenslet on top of a substrate. (b) Rectangular section before reflow (top) and corresponding lens section after reflow (bottom) with the lenslet parameters: S_{circ}: surface of lenslet section above the substrate, R: radius of curvature, w: width of lenslet, h: sag-height, f: focal length, d: mono-lens substrate thickness.

The solution for the radius R is:

$$R = \frac{-b - \sqrt{b^2 - 4ac}}{2a} \quad with \quad \begin{aligned} a &= 4m^2 - 8m \\ b &= 8d(1-m) \\ c &= w^2 + 4d^2 \end{aligned} \tag{8}$$

Optics EXPRESS

As explained further in Section 5., we fabricate the cylindrical lenslets by reflow of the resist. The height and width of the deposited resist defines the shape of the lens section (Fig. 7(b)). In order to determine the rectangular section S_{rect} of the resist material to be deposited, one needs to calculate the surface S_{circ} of the circular segment of the lens above the substrate.

To obtain the surface of the circular lens segment, one subtracts the surface of the triangle from the surface of the disk segment (Fig. 7(b)).

$$S = 2\left(\frac{R^2\theta}{2} - \frac{\frac{w}{2}\cdot(R-h)}{2}\right) \tag{9}$$

and since $R - h = R\cos\theta$ and $w/2 = R\sin\theta$, we obtain

$$S = R^2\theta - R^2\sin\theta\cdot\cos\theta \tag{10}$$

and after simplifying

$$S = \frac{R^2}{2}(2\theta - \sin(2\theta)) \tag{11}$$

where $\theta = \arcsin(w/(2R))$. Recommended rectangular resist profiles before reflow have a height that is lower than the sag-height of the desired lenslet [19].

Using these equations, one can calculate the lens parameters to be used to obtain the desired focal length of the revealer for a given lens width. Similar parameters define the size of the considerably smaller base layer lenslets located within the base layer shapes. Note that depending on design and fabrication considerations, the repetition period T_r may be slightly larger than the lenslet width w_r.

Another possibility of creating a strong contrast between base layer shape interior and exterior consists in selecting one orientation and a standard repetition period for the cylindrical lenslets inside and another orientation and a small period for the cylindrical lenslets outside the base layer shapes (Fig. 8(d)). The cylindrical lenslet grating with the small repetition period that covers the shape background (exterior region) incorporates structures whose dimensions are a few multiples of the wavelength of the visible light. They diffract the incident light. When tilting the device

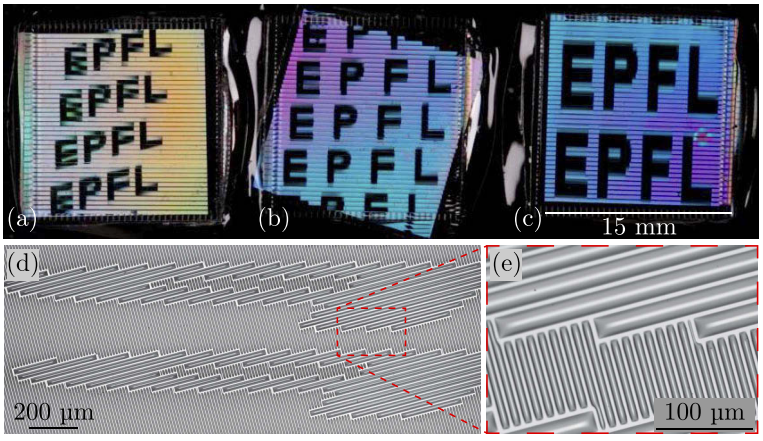

Fig. 8. Diffracting 1D moirés formed by a horizontal revealer lenslet grating of repetition period 400 µm, of base layer shape foreground (inside) lenslets of period (a) 16 µm horizontal, (b) 27 µm at 15°, (c) 27 µm horizontal and of base layer shape background (outside) lenslets of period (a) 8 µm vertical, (b) 12 µm at 105°, and (c) 12 µm vertical. (d) Optical micrograph of the letter "P" within the base of (b), where the text in the base is mirrored to obtain a correctly-oriented text when looking through the revealer. (e) Magnified area of (d).

Optics EXPRESS

along an axis having the same orientation as this background lenslet grating, the background appears as changing colors. Since the foreground cylindrical lenslets of the base are more than twice as large, they do not significantly diffract light and a strong contrast is created (Figs. 8(a), 8(b), and 8(c)).

5. Fabrication of cylindrical lenslets

The cylindrical lenslets that have to be placed on both sides of a transparent substrate are fabricated in a similar manner as the spherical lenslets that have been described in the literature [20,21]. The process flow (Fig. 9) is divided in two parts. We first create a master for each lens layout. Then, we replicate these designs on the two sides of a transparent substrate. The fabrication was carried out as described below because of the flexibility of the process and the relative ease of fabricating samples quickly. In further developments, other processes could be used if different constraints are considered. The fabrication could be for example based on dry etching into glass, on hot embossing, or on roll-to-roll embossing.

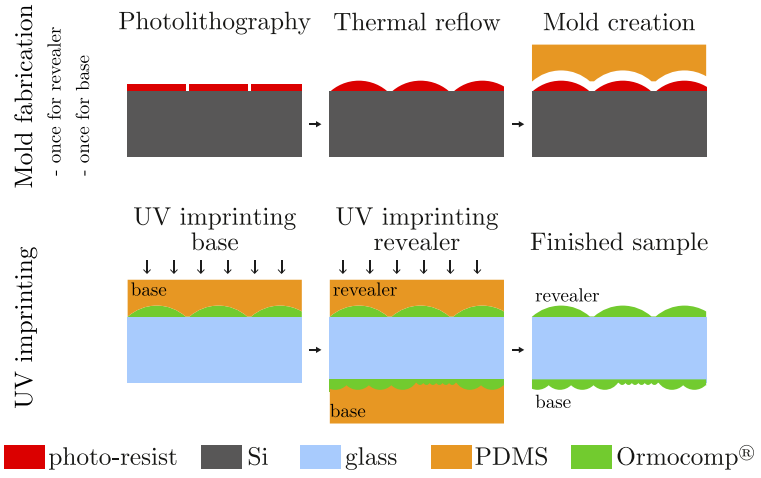

Fig. 9. Process flow for the micro-fabrication of the lenslet gratings.

5.1. Creation of the masters

A clean silicon wafer is treated with hexamethyldisilazane (HMDS) before photo-resist spin-coating. The spin-coating parameters and the photo-resist are selected in order to obtain the desired film thickness. This thickness will determine the final shape of the lenslets. The spin-coated wafers are then soft-baked and locally exposed to UV radiation by direct laser writing. After exposure, the patterns are developed, rinsed and dried. In order to obtain a circular shape profile, we apply a thermal reflow technique. By heating up the wafer above the glass-liquid transition temperature of the resist ($\approx 120^{\circ}$ C), due to surface tension, the rectangular cuboids made of resist start to have a more circular profile. Once the wafer cools down, the cylindrical lens shapes harden. We obtain a master for the shapes of the lenslets that will be placed on one side of the target transparent substrate. The same process is carried out for the lenses that need to be placed on the other side of the substrate.

5.2. Creation of the molds

A polydimethylsiloxane (PDMS) mold is fabricated for each master, according to the standard molding process. The surface of the masters is silanized to facilitate the release of the PDMS

Optics EXPRESS

from the surface of the master. The PDMS is prepared by mixing 10 parts of PDMS monomers and 1 part of curing agent. After mixing, the PDMS is poured onto the masters and is degassed in a desiccator. When all the bubbles have disappeared, the PDMS is cured for two hours at 80° C and then peeled off of the master. We thus obtain the molds with which the lenses are produced on each side of the transparent substrate.

5.3. Replication of the lenslets onto the target substrate

The replication of the master onto the transparent substrate is done by UV imprinting. We use a UV-curable resin (OrmoComp) to fill the molds and press them against a microscope slide or a glass wafer. By exposing the resin to UV radiations, it cross-links and can subsequently be detached from the molds.

In this replication step, the most critical aspect is the alignment of the two molds on the substrate. This is achieved visually thanks to the moiré itself, which can be seen through the mold and the substrate. Since the moiré is very sensitive to misalignments, we have a direct visual feedback that enables us to align the layers properly to obtain the desired moiré effect. Misalignments can nonetheless happen during the imprinting or when placing the substrate and the mold in the UV-imprinter and could be improved in a future redesign of the tool.

6. Realisations

To obtain moiré samples that are visible and visually appealing, the trade-offs between the different parameters must be understood. The notations used in the following explanations are the same as those described in Section 2.2. For a fixed base and a horizontal revealer, when the revealer is translated vertically on top of the base, the speed of the moiré is equal to $\frac{\|\vec{p}\|}{T_r}$ times the speed of the revealer. Therefore, fast moiré displacements are obtained with small periods T_r of the revealer and for large moiré tiles (large vertical moiré replication component p_y). The moiré repetition vector is also related to the size of the base bands: $\vec{p} = \frac{T_r}{T_r - t_y}\vec{t}$. When $t_y < T_r$, the moiré moves opposite to the revealer movement. For a given moiré repetition vector, the smaller the period of the revealer, the smaller the base bands. Some problems may arise when the base band period t_y becomes too small. Since the shapes in the base are filled with lenslets (Fig. 5(d)), their dimensions must be large enough. This limitation starts becoming visible in Fig. 11 where the base bands that correspond to the "valid" are smaller than those of the "ok" and are therefore less well-resolved. The period of the revealer dictates the focal lengths that can be achieved. For a given period, only a limited range of radii of curvature can be achieved. This limits the focal length of the revealer and therefore limits the thickness of the overall sample. For a given range of tilt angles, to obtain moiré displacements that are large in respect to the moiré size, the period of the revealer should be small and the sample thin. The corresponding base bands are also small and their base band shapes will be harder to fill with lenslets.

Another important aspect of the fabrication is the alignment between the base and the revealer. Since the moirés are sensitive to small displacements or rotations, any misalignment is easily detectable visually once the sample is fabricated. A translation that is parallel to the orientation of the revealer lenses has no impact on the moiré. A translation Δy perpendicularly to the revealer lenses results in a translation of the moiré by $\frac{\Delta y}{T_r} \cdot \vec{p}$.

Let us analyze the effect of an undesired rotation of the revealer that may occur at fabrication time. Such a rotation results in a linear deformation of the moiré. To explore the effect of this rotation, we develop Eq. (2) by defining the rotation of the revealing layer as revealing layer transformation, i.e. $g_y(x_t, y_t) = -sin\theta \cdot x_t + cos\theta \cdot y_t$. Since the base layer is not changed, the transformation applied to the base layer is the identity transformation, i.e. $h_x(x_t, y_t) = x_t$ and $h_y(x_t, y_t) = y_t$. The development of Eq. (2) yields the matrix M_t expressing the transformation

Optics EXPRESS

from transformed space (x_t, y_t) to original space (x, y) of the moiré layer, for a rotation angle θ:

$$\begin{bmatrix} x \\ y \end{bmatrix} = M_t \cdot \begin{bmatrix} x_t \\ y_t \end{bmatrix} \tag{12}$$

with

$$M_t = \frac{1}{T_r - t_y} \begin{bmatrix} T_r - t_y + t_x \cdot sin\theta & t_x(1 - cos\theta) \\ t_y \cdot sin\theta & T_r - t_y \cdot cos\theta \end{bmatrix} \tag{13}$$

By inverting matrix M_t, we deduce the positions of points within the moiré space after rotation as a function of their position before the rotation. Thus

$$\begin{bmatrix} x_t \\ y_t \end{bmatrix} = M_t^{-1} \cdot \begin{bmatrix} x \\ y \end{bmatrix} \tag{14}$$

with

$$M_t^{-1} = \frac{T_r - t_y}{(T_r - t_y + t_x \cdot sin\theta)(T_r - t_y \cdot cos\theta) - t_x(1 - cos\theta)t_y \cdot sin\theta} \cdot \begin{bmatrix} T_r - t_y \cdot cos\theta & -t_x(1 - cos\theta) \\ -t_y \cdot sin\theta & T_r - t_y + t_x \cdot sin\theta \end{bmatrix} \tag{15}$$

In the case of the moiré depicted in Fig. 11, the effect of the rotation of the revealer on the moiré is shown in Fig. 10.

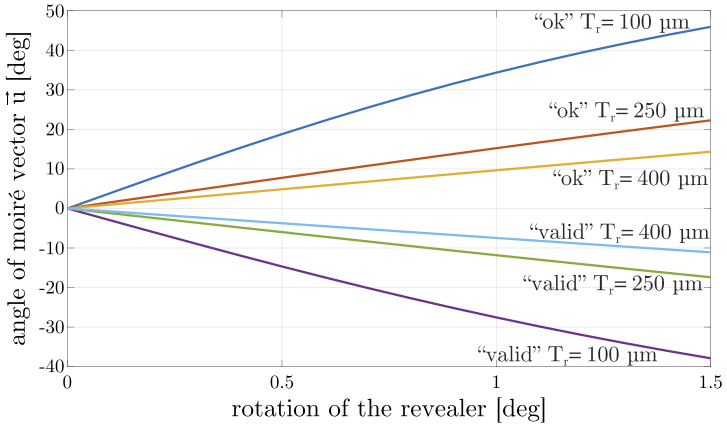

Fig. 10. Effect of the rotation of the revealer on a horizontal moiré vector ($\vec{u}$ in Fig. 4). The considered moirés are the "ok" and the "valid" moirés shown in Fig. 11. For each curve, the base layer size has been calculated to yield the same moiré size. Even small rotations of the revealer have a large impact on the moiré shapes. We can also observe that the smaller the period T_r of the revealer, the larger the impact that misalignments have on the moiré.

Realisations of the 1D-moiré by lenslets comprise an "EPFL" moiré which moves diagonally (see Visualization 2). As shown in Fig. 8, at some illumination and viewing angles, the contrast between moiré shape foreground and background is obtained by the diffractive colors of the background that are produced by the small lenticular gratings with repetition periods between 8

Optics EXPRESS

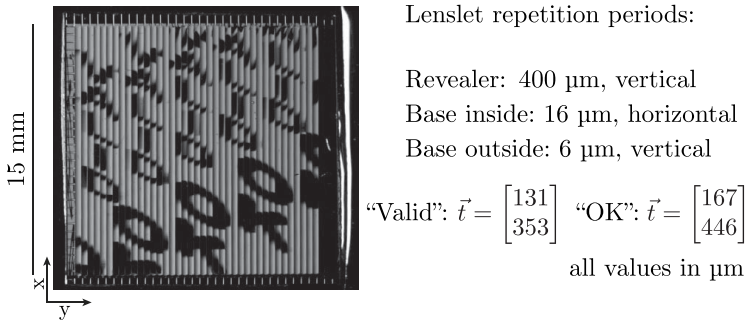

Fig. 11. Capture of the "VALID" and "OK" 1D lenslet grating moiré moving in opposite directions, see the video (Visualization 3).

µm and 12 µm. Under other illumination and viewing conditions, instead of diffractive colors there is an intensity contrast similar to the ones shown in Figs. 11, 13, and 14.

One may also create a design that comprises two distinct lenslet 1D moirés that move in different directions and that have different base layer layout parameters. In the design shown in Fig. 11, the "Valid" and "OK" 1D moirés move in opposite directions (Visualization 3).

We also fabricated curvilinear moirés that are laid out according to the equation establishing the relations between the geometric transformation of the base layer, the geometric transformation of the revealing layer and the geometric transformation of the corresponding moiré image (Eq. (2)). Let us assume a desired geometric transformation of the moiré layer $x = m_x(x_t, y_t), y = m_y(x_t, y_t)$, where (x_t, y_t) and (x, y) express the coordinates in the transformed and original space, respectively.

Then, from Eq. (2) we derive the corresponding geometric transformation of the base layer:

$$\begin{aligned} h_x(x_t, y_t) &= \big(g_y(x_t, y_t) - m_y(x_t, y_t)\big) \cdot \frac{t_x}{T_r} + m_x(x_t, y_t) \\ h_y(x_t, y_t) &= g_y(x_t, y_t) \cdot \frac{t_y}{T_r} + m_y(x_t, y_t) \cdot \frac{T_r - t_y}{T_r} \end{aligned} \tag{16}$$

where (t_x, t_y) is the base band repetition vector in the original space, T_r is the revealing lenslet grating repetition period in the original space and $g_y(x_t, y_t)$ expresses the geometric transformation of the revealing layer from transformed to original space.

A desired geometric transformation, for example a circularly laid out moiré, is expressed by Eq. (17) that brings (x_t, y_t) positions within the transformed space into (x, y) positions within the original non-transformed space:

$$\begin{aligned} x &= m_x(x_t, y_t) = \frac{\pi - \arctan(y_t - c_y, x_t - c_x)}{2\pi} w_x \\ y &= m_y(x_t, y_t) = c_m \sqrt{(x_t - c_x)^2 + (y_t - c_y)^2} \end{aligned} \tag{17}$$

where the function $\arctan(y, x)$ returns the angle α of a radial line of slope y/x, with the returned angle $\alpha \in [-\pi; \pi]$, where constant c_m expresses a scaling factor, and constants c_x and c_y give the center of the circular moiré image layout in the transformed moiré space. The moiré text in the original space (x, y) is formed by the original non-transformed horizontally laid out text of width w_x, which upon tilting the device moves vertically. In the transformed space (x_t, y_t), the moiré text message is laid out circularly and the equivalent of the vertical movement is a radial movement.

By inserting $m_x(x_t, y_t)$ and $m_y(x_t, y_t)$ into Eq. (16), we obtain geometric transformation (18) from transformed space to original space that is used to create the base layer in the transformed

Optics EXPRESS

space:

$$h_x(x_t, y_t) = \left(y_t - c_m\sqrt{(x_t - c_x)^2 + (y_t - c_y)^2}\right)\frac{t_x}{T_r} + \frac{\pi - \arctan(y_t - c_y, x_t - c_x)}{2\pi}w_x$$
$$h_y(x_t, y_t) = c_m\sqrt{(x_t - c_x)^2 + (y_t - c_y)^2}\frac{T_r - t_y}{T_r} + y_t\frac{t_y}{T_r} \tag{18}$$

We apply, pixel by pixel, the base layer transformation (18) from transformed space to original space and transfer the color of the pixel in the original space to the corresponding pixel in the transformed space. We obtain the transformed base layer layout shown in Fig. 12(a).

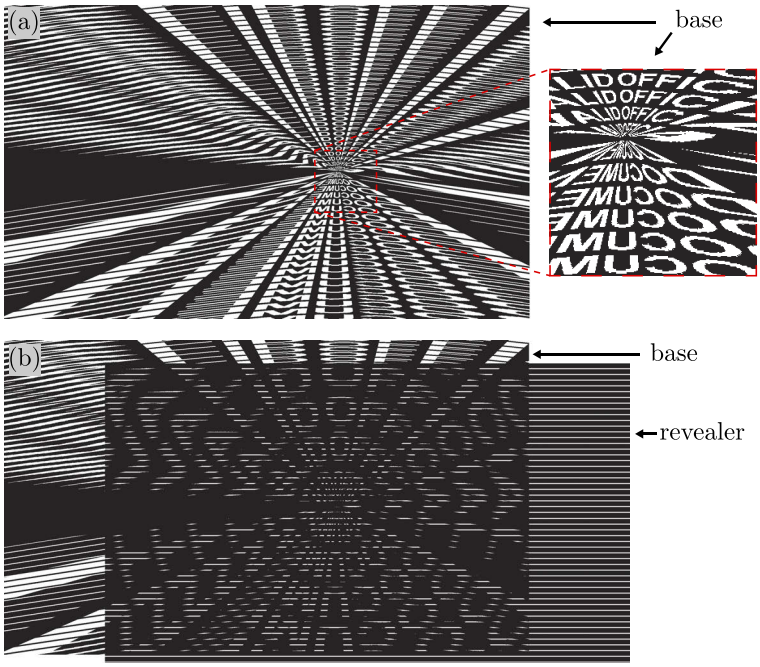

Fig. 12. (a) Base layer design in which the white areas correspond to the interior of the shapes and the black areas correspond to the outside. From this design, the base can be filled with lenslets. (b) Superposition of the base and the revealer to visualize the message formed by the moiré. This specific moiré design was used to fabricate the sample shown in Fig. 13(a).

The base lenslet layer is obtained by fabricating inside the base layer shapes (white areas in Fig. 12) lenslet gratings of 16 µm repetition period oriented at 15° and outside them randomly-placed spherical lenslets of 4 to 7 µm diameter. The revealing lenslet layer is obtained by fabricating a horizontal lenslet grating having a repetition period of 400 µm. The 15° orientation of the base ensures that no undesired interference occurs with the revealer. The resulting lenslet grating device is shown in Fig. 13. Observe also the video where the circular moiré is evolving radially (Visualization 4).

A similar approach is applied for creating petals rotating circularly when tilting the lenslet device. One part of a frame from the video (Visualization 5) is shown in Fig. 14.

Optics EXPRESS

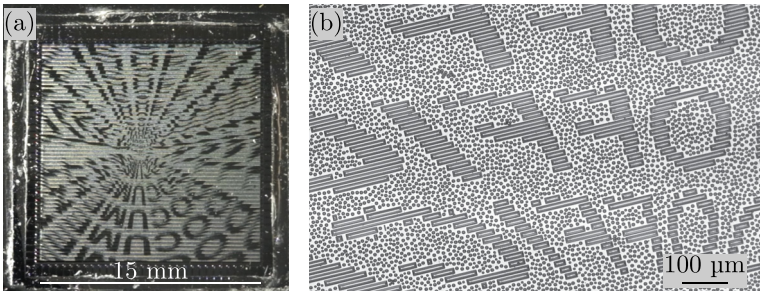

Fig. 13. (a) Part of frame extracted from the video showing the tilted lenslet device (Visualization 4). (b) Optical micrograph of an area of the base. The interior of the shapes is filled with rectilinear cylindrical lenses of period 16 µm at 15°. The exterior of the shapes is filled with randomly-placed spherical lenslets.

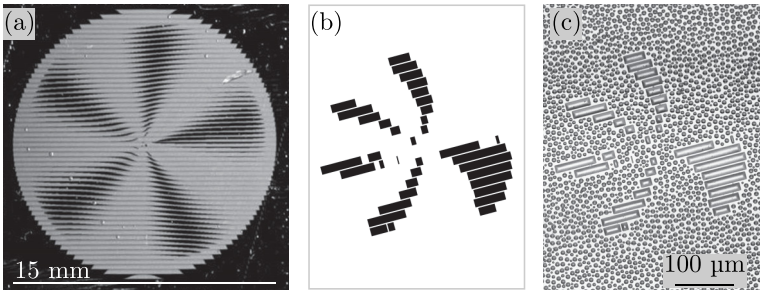

Fig. 14. (a) Part of frame extracted from the video showing the tilted lenslet device (Visualization 5). (b) Bitmap showing the lens layout in the center of the design. The black lines indicate the place of the cylindrical lenslets. (c) Optical micrograph of the fabricated lenslet base layer. The interior of the shapes is filled with rectilinear cylindrical lenses of period 16 µm at 15°. The exterior of the shapes is filled with randomly-placed spherical lenslets.

7. Conclusions

We observed that two superposed layers of lenslet gratings, illuminated from behind by dark-bright or multi-colored light creates well-contrasted classical moiré fringes. The top lenslet grating, called revealing layer, samples the underlying illumination patterns that are created within its focal plane. The bottom lenslet grating, called base layer, creates these illumination patterns.

Relying on this observation, we aimed at progressing beyond the classical moiré fringes and created visually interesting optical effects such as rectilinear 1D moirés and geometrically-transformed curvilinear moirés.

Rectilinear and curvilinear 1D moirés are produced by fabricating superposed lenslet gratings. The necessary cylindrical lenslets are fabricated by applying lithographic techniques to generate the rectangular resist profiles. By heating the material, thanks to the reflow process, the rectangular lenslet profile becomes circular. Molds are then created and used to UV-imprint the lens shapes on both sides of a transparent substrate. Upon tilting of the fabricated lenslet device, symbols, graphical elements or variable intensity images become animated. The revealer is generally composed of a rectilinear cylindrical lenslet array. The base layer requires an arrangement of lenslets that creates a strong contrast between the interior (foreground) and exterior (background) of the tiny replicated base layer shapes. An excellent contrast is offered by small cylindrical lenslet gratings in the shape foreground (typically 16 µm repetition period, with 15° orientation)

Optics EXPRESS

and very small cylindrical lenslet gratings in the shape background (typically 8 to 12 μm repetition period, with 105° orientation). This excellent contrast is due to the diffraction of light across the very small background gratings, thereby creating varying colors. One may also create a high contrast without color-varying effects by placing small spherical lenslets of diameters varying between 4 to 7 μm at random locations in the shape background. These randomly-placed small spherical lenslets diffuse the light coming from the back and create a contrast with the larger cylindrical lenslet gratings of the shape foreground that direct light from a specific orientation across the revealer cylindrical lenslet grating towards the viewer. Upon tilting the 1D lenslet device, graphic symbols or text move upwards, sideways, diagonally, or in a radial manner.

Applications relying on moiré images produced by superposed lenslet gratings are numerous. A privileged domain of application is document security. Lenslet gratings can for example be integrated as visual security elements onto the transparent windows that are often present in today's banknotes and identity cards. The small dimensions of the lenslets as well as their unknown layout parameters make them very difficult to replicate and therefore adequate for the prevention of counterfeits. Although beyond the scope of this article, it is also possible to apply encapsulating layers to prevent any replication of the final micro-lenses.

Lenslet grating moirés can also be used for decoration and publicity. They can be as large as desired and be placed as decorative elements on plastic or glass. People walking in front of such gratings illuminated from the back may observe the dynamically-evolving moirés induced by their change of position. The lenslet grating moiré technology therefore offers great promises for art, security, and decoration.

Acknowledgments

The authors thank the staff of the EPFL Center of Micronanotechnology (CMi) for their valuable help and thank École Polytechnique Fédérale de Lausanne for its support.

Disclosures

TW: EPFL (P), TB: EPFL (P), VF: EPFL (P), RDH: EPFL (P, I), JB: EPFL (P). The authors declare no conflict of interest.

References

1. G. Oster, "Optical art," Appl. Opt. **4**(11), 1359–1369 (1965).
2. G. Lebanon and A. M. Bruckstein, "Variational approach to moiré pattern synthesis," J. Opt. Soc. Am. A **18**(6), 1371–1382 (2001).
3. R. D. Hersch and S. Chosson, "Band moiré images," ACM Trans. Graph. (Proc. Siggraph) **23**(3), 239–247 (2004).
4. V. J. Cadarso, S. Chosson, K. Sidler, R. D. Hersch, and J. Brugger, "High-resolution 1d moirés as counterfeit security features," Light: Sci. Appl. **2**(7), e86 (2013).
5. R. Steenblik, M. Hurt, and G. Jordan, "Micro-optic security and image presentation system," (2008). US Patent 7,333,268.
6. A. Righi, "Sui fenomeni che si producono colla sovrapposizione di due peticoli e sopra alcune loro applicazioni," Il Nuovo Cimento (1877-1894) **21**(1), 203–228 (1887).
7. D. Tollenaar, *Moiré: interferentieverschijnselen bij rasterdruk, Moiré interference phenomena in halftone printing English translation published in 1964, reprinted in Indebetouw G. Czarnek R. (Eds.). Selected Papers on Optical Moiré and Applications, SPIE Milestone Series, Vol. MS64, 1992, pp. 618-633* (Instituut voor Grafische Techniek, 1945).
8. Y. Nishijima and G. Oster, "Moiré patterns: Their application to refractive index and refractive index gradient measurements," J. Opt. Soc. Am. **54**(1), 1–5 (1964).
9. O. Bryngdahl, "Moiré: Formation and interpretation," J. Opt. Soc. Am. **64**(10), 1287–1294 (1974).
10. I. Amidror, *The Theory of the Moiré Phenomenon - Volume I: Periodic Layers* (Springer-Verlag, 2009), 2nd ed.
11. M. C. Hutley, R. Hunt, R. F. Stevens, and P. Savander, "The moire magnifier," Pure Appl. Opt. **3**(2), 133–142 (1994).
12. J. A. Hala Kamal and Reinhard Voelkel, "Properties of moire magnifiers," Opt. Eng. **37**(11), 3007–3014 (1998).
13. O. Mikami, "New image-rotation using moiré lenses," Jpn. J. Appl. Phys. **14**(7), 1065–1066 (1975).
14. I. Amidror, "A generalized fourier-based method for the analysis of 2d moiré envelope-forms in screen superpositions," J. Mod. Opt. **41**(9), 1837–1862 (1994).

Optics EXPRESS

15. S. M. Chosson and R. D. Hersch, "Beating shapes relying on moiré level lines," ACM Trans. Graph. **34**(1), 1–11 (2014).
16. W. Zheng, S. Shen, Y. Gao, N. Liu, and Y. Liu, "Design methodology for moiré magnifier based on micro-focusing elements," Opt. Express **25**(25), 31746–31757 (2017).
17. T. Walger, T. Besson, V. Flauraud, R. D. Hersch, and J. Brugger, "Level-line moirés by superposition of cylindrical micro-lens gratings; submitted to josa-a," JOSA-A (2019).
18. E. Hecht, *Optics, Chapter 5* (Pearson, 2017), 5th ed.
19. P. Nussbaum, R. Völkel, H. P. Herzig, M. Eisner, and S. Haselbeck, "Design, fabrication and testing of microlens arrays for sensors and microsystems," Pure Appl. Opt. **6**(6), 617–636 (1997).
20. Z. D. Popovic, R. A. Sprague, and G. A. N. Connell, "Technique for monolithic fabrication of microlens arrays," Appl. Opt. **27**(7), 1281–1284 (1988).
21. D. Daly, R. F. Stevens, M. C. Hutley, and N. Davies, "The manufacture of microlenses by melting photoresist," Meas. Sci. Technol. **1**(8), 759–766 (1990).